International Journal of Pharmaceutics 375 (2009) 123–132

Contents lists available at ScienceDirect

International Journal of Pharmaceutics

journal homepage: www.elsevier.com/locate/ijpharm

Pharmaceutical Nanotechnology

Low molecular weight chitosan in DNA vaccine delivery via mucosa

Xiaorong Yang, Xiying Yuan, Danning Cai, Shaoying Wang, Li Zong*

Institute of Pharmaceutics, School of Pharmacy, China Pharmaceutical University, Tong Jia Xiang 24, Nanjing 210009, Jiangsu, People's Republic of China

ARTICLE INFO

Article history:
Received 17 September 2008
Received in revised form 20 March 2009
Accepted 28 March 2009
Available online 5 April 2009

Keywords:
Chitosan
Low molecular weight
DNA vaccine
Mucosa
Intranasal immunization

ABSTRACT

It is acknowledged that low molecular weight chitosan (LMWC) is advantageous over high molecular weight chitosan (HMWC) in the biodegradability. In this report, the potential of LMWC in DNA vaccine delivery via mucosa was evaluated. Firstly, the effects of molecular weight of chitosan on the physicochemical properties and *in vitro* transfection efficiency of chitosan/DNA polyplexes were investigated. Secondly, the capabilities of the polyplexes based on LMWC to elicit serum IgG antibodies and to attenuate the development of atherosclerosis after intranasal vaccination were compared with the polyplexes based on HMWC in the rabbit model. Finally, the intramucosal transport of the double-labeled polyplexes was observed by confocal microscopy. The results indicated that LMWC had lower binding affinity to DNA and mediated higher transfection efficiency. Intranasal vaccination with LMWC/DNA polyplexes could elicit significant systemic immune responses, modulate the plasma lipoprotein profile and attenuate the progression of atherosclerosis. Those aspects were comparable to those obtained by HMWC/DNA polyplexes. As revealed by confocal images, LMWC/DNA polyplexes remained stable during interaction with the nasal mucosa, and were internalized by nasal epithelial cells, which was similar to the case of HMWC/DNA polyplexes. In conclusion, LMWCs have potential applications in DNA vaccine delivery via mucosa.

1. Introduction

The major challenge in gene therapy is to develop safe and efficient vehicles that deliver exogenous DNA into target cells to achieve desired expression of the encoded protein. Chitosan has been particularly appealing as a non-viral carrier for gene delivery in recent years because of its unique properties, such as biocompatibility, biodegradability and low cytotoxicity (Guliyeva et al., 2006; Özgel and Akbuğa, 2006). Protonated chitosan in acidic environment could condense negatively charged DNA into nanoscale polyplexes through electrostatic interaction. These polyplexes could provide efficient protection of DNA against nuclease degradation and deliver DNA into target cells via endocytosis. However, compared with high transfection efficiency of the viral vector, the transfection efficiency mediated by chitosan *in vitro* is still relatively low (Chae et al., 2005b; Mansouri et al., 2006). The molecular weight (MW) of chitosan, ranging from several thousands to millions of Daltons, has been proven to be one of the most important factors that influence the gene expression (Romøren et al., 2003; Lavertu et al., 2006). However, the *in vitro* transfection efficiencies obtained by various research groups did not indicate whether the high or low molecular weight chitosan is more suitable for gene delivery (Lee et al., 2001; Huang et al., 2005; Köping-Höggård et al., 2004; Zhao et al., 2006). Our findings showed that the low molecular weight chitosan (LMWC) mediated higher transfection efficiency *in vitro* than did the high molecular weight chitosan (HMWC).

Biodegradability and low cytotoxicity are the most important advantages of LMWCs over other gene carriers. It was reported that the HMWC degraded slowly *in vivo*, and there was a consequential risk of accumulation in the tissues in a long period of administration (Nakamura et al., 1992). However, shorter-chain LMWCs was easily degraded to smaller oligo- and mono-saccharides, which were subsequently excreted as carbon dioxide (MacLaughlin et al., 1998). Moreover, there were MW-dependent cytotoxic effects in the application of chitosans (Carreño-Gómez and Duncan, 1997; Chae et al., 2005a), and the majority of the publications indicated that LMWC showed negligible cytotoxic effect in various cell lines (Richardson et al., 1999; Kim et al., 2004; Chae et al., 2005a). Furthermore, the drawbacks associated with HMWC, such as high viscosity and insolubility at physiological pH, could partially be circumvented by using water soluble LMWC (Köping-Höggård et al., 2003, 2004).

Recently, mucosal immunization has attracted more attention due to an increasing patient compliance, less painful administration and efficient induction of both humoral and cellular immune responses. One of the approaches to improve the transport of DNA vaccine across the epithelial barriers is to design DNA-loaded chitosan nanoparticles. Conventional HMWCs (>100 kDa) have already

* Corresponding author. Tel.: +86 25 85231173; fax: +86 25 83271335.
E-mail address: zong216@yahoo.com.cn (L. Zong).

0378-5173/$ – see front matter © 2009 Elsevier B.V. All rights reserved.
doi:10.1016/j.ijpharm.2009.03.032

been used as carriers to deliver DNA vaccines via oral, nasal and pulmonary route and induce effective immune responses (Bivas-Benita et al., 2004; Zhang et al., 2007; Khatri et al., 2008). However, at present, there are only limited *in vivo* data available for LMWC (<10 kDa) as gene carriers and the effect of chitosan MW on efficacy of *in vivo* gene delivery.

Human cholesteryl ester transfer protein (CETP), a 74 kDa plasma glycoprotein, plays an important role in lipid metabolism, through mediating the exchange of cholesteryl ester and triglyceride between lipoproteins. The inhibition of CETP activity by vaccine-induced antibodies contributes to the increase in plasma high density lipoprotein cholesterol (HDL-C) and the decrease in plasma low density lipoprotein cholesterol (LDL-C), which is considered to be a promising method in the treatment of atherosclerosis (Nilsson et al., 2005; Barter and Kastelein, 2006). In the previous study, we had constructed an immunotherapeutic DNA vaccine encoding cholesteryl ester transfer protein C-terminal fragment (CETP-C) displayed by Hepatitis B virus core particle (Mao et al., 2006). It was found that the intranasal immunization of the CETP vaccine formulated with HMWC could induce anti-CETP antibodies and inhibited the development of atherosclerosis in a rabbit model (Yuan et al., 2008). Thus, the potential application of LMWC as a carrier for *in vivo* delivery of the DNA vaccines was investigated in this study. Firstly, DNA was complexed with chitosan to form chitosan/DNA polyplexes, and the effect of chitosan MW (5, 8, 32, 173 and 425 kDa) on the physicochemical properties and *in vitro* transfection efficiency of the chitosan/DNA polyplexes was evaluated. Following that, in a high-cholesterol rabbit model, we initiated a specific immunotherapy through nasal administration of DNA vaccine against CETP and assessed the potentials of the LMWC/DNA polyplexes to elicit serum anti-CETP IgG antibodies, to modulate the plasma lipoprotein profile and to attenuate the atherosclerosis development. Finally, the influence of chitosan MW on the transport of polyplexes across the nasal mucosa was investigated using rhodamine B isothiocyanate (RBITC)-labeled chitosan and fluorescein isothiocyanate (FITC)-labeled DNA by the confocal laser scanning microscopy (CLSM).

2. Materials and methods

2.1. Materials

Chitosans of 5, 8, 32, 173 and 425 kDa with the same deacetylation degree of 95.5% were supplied by Shanghai KABO Trading Co. Ltd., China. The plasmid pEGFP-C3 encoding green fluorescent protein was obtained from Clontech, USA. The plasmid DNA encoding CETP-C was a generous gift from Minigene Pharmacy Laboratory of China Pharmaceutical University (Nanjing, China). Two plasmid DNA were amplified in *Escherichia coli* DH5α and purified using Qiagen Plasmid Maxi Kit (Qiagen, Germany). Fetal bovine serum (FBS) was purchased from Hyclone, USA. Dulbecco's modified Eagle medium (DMEM) and trypsin were obtained from Gibco, USA. Hoechst 33258 and fluorescein isothiocyanate (FITC) were acquired from Sigma, USA. Rhodamine B isothiocyanate (RBITC) was purchased from Serva, USA. Horseradish peroxidase (HRP)-conjugated goat anti-rabbit IgG was purchased from Promega, USA. Total cholesterol (TC), HDL-C and LDL-C kits were obtained from Wako, Japan. All other chemicals and reagents were obtained from commercial sources with the highest purity available.

2.2. Preparation of chitosan/DNA polyplexes

The chitosan/DNA polyplexes were prepared at N/P (amino to phosphate groups) ratio of 5 by a complex coacervation technique. Briefly, chitosans of various MW (5, 8, 32, 173 and 425 kDa) were dissolved in 5 mM acetate buffer (pH 5.5) to 500 μg/ml, respectively. A chitosan solution and a DNA solution of 200 μg/ml in 5 mM sodium sulfate solution were separately preheated to 50 °C. Equal volumes of the two solutions were mixed and immediately vortexed for 30 s. The resulted polyplexes were left to stand for at least 30 min at room temperature before use.

2.3. Characterization of chitosan/DNA polyplexes

The particle size and zeta potential of the chitosan/DNA polyplexes prepared with chitosans of various MW were analyzed by a 3000HSA Zetasizer (Malvern, UK). In assay of the association efficiency of DNA, the chitosan/DNA polyplexes suspension was first centrifuged (3K30, Sigma, USA) at 30,000 × *g*, 4 °C for 30 min. The amount of free DNA in the supernatant was then analyzed using the Hoechst 33258 dye with a spectrofluorophotometer (RF5301PC, Shimadzu, Japan) at excitation and emission wavelengths of 351 and 454 nm, respectively. The association efficiency (AE) was calculated as follows:

$$\mathrm{AE}\,(\%) = \frac{\mathrm{DNA_{total}} - \mathrm{DNA_{free}}}{\mathrm{DNA_{total}}} \times 100,$$

where $\mathrm{DNA_{total}}$ is the total amount of DNA; $\mathrm{DNA_{free}}$ is the amount of free DNA in the supernatant.

2.4. In vitro release of DNA

A volume of 4 ml of chitosan/DNA polyplexes was dispersed in 30 ml of phosphate buffered saline (PBS, pH 7.4). The suspension was incubated at 37 °C in a shaking incubator at 180 rpm. After 0, 4, 12, 24, 36, 48 and 60 h incubation, a series of 1 ml of samples were withdrawn and centrifuged at 30,000 × *g*, 4 °C for 30 min. The amount of free DNA in the supernatant was determined by fluorospectrophotometry. The cumulative release of DNA was calculated.

2.5. Gel retardation assay

The stability of the chitosan/DNA polyplexes was evaluated using gel retardation assay. The polyplexes prepared with chitosans of various MW and the naked DNA were electrophoresed on 0.8% agarose gel containing 0.5 mg/ml of ethidium bromide for 60 min at a constant voltage of 100 V. The DNA bands were visualized and photographed using the UV-transilluminator (TMW-20, UVP Inc., USA).

2.6. DNase I protection assay

The capability of chitosans with different MW to protect DNA from nuclease degradation was studied by agarose gel electrophoresis. The chitosan/DNA polyplexes prepared with 5, 32, 173, and 425 kDa chitosans (20 μl, equivalent to 2 μg of DNA) were incubated with DNase I of 60 unit/ml for 30 min at 37 °C, respectively. As a control, 20 μl of naked DNA solution (equivalent to 2 μg of DNA) was incubated with DNase I of the same concentration. The reaction was terminated by adding iodoacetic acid. The integrity of DNA was then analyzed by 0.8% agarose gel electrophoresis as described above.

The effect of 5 kDa chitosan on protection of DNA against nuclease degradation was evaluated by incubating 5 kDa chitosan-based polyplexes (20 μl, equivalent to 2 μg of DNA) with serial dilution of DNase I ranging from 5 to 25 unit/ml for 30 min at 37 °C. The samples were applied to agarose gel electrophoresis as described above. Untreated polyplexes and DNA, DNA treated with 5 unit/ml of DNase I were used as controls.

2.7. In vitro transfection

The plasmid DNA encoding green fluorescent protein (pEGFP-C3) was used as a reporter gene to evaluate the *in vitro* transfection efficiency. The human embryonic kidney cells (HEK293 cells), donated by the National Drug Screening Center of China Pharmaceutical University (Nanjing, China), were grown in DMEM supplemented with 10% FBS, 100 mg/ml streptomycin and 100 unit/ml penicillin at 37 °C in a humidified 5% carbon dioxide incubator (Thermo, Forma, USA). Cells were seeded into 24-well plates at a density of 2×10^5 cells per well and were incubated for 18–24 h to achieve approximately 60–80% confluence. For FBS-free condition, the medium was replaced by 400 μl of FBS-free DMEM before transfection. The polyplexes (equivalent to 4 μg of DNA) were added to each well and then incubated with HEK293 cells for 4 h at 37 °C. The transfection medium was removed and replaced with a fresh DMEM containing 10% FBS. The cells were further incubated for 40 h, and then washed with cold PBS and harvested by using trypsin solution. The cell suspension was centrifuged at $1800 \times g$ for 5 min and resuspended in 0.5 ml of PBS. Transfection efficiency was analyzed by a flow cytometer (Becton Dickinson, USA). The naked DNA solution was used as a control (mean ± S.D., $n = 4$).

2.8. DNA immunization procedure and rabbit cholesterol-fed atherosclerosis model

LMWC (5 kDa) and HMWC (173 kDa) were chosen to compare the difference in gene delivery efficacy *in vivo*. LMWC/DNA and HMWC/DNA polyplexes were prepared as described above. The polyplexes were lyophilized (SD-1, Beijing Boyikang Lab. Instrument, Beijing, China) in the presence of mannitol and lactose. The lyophilized polyplexes were resuspended in sodium acetate buffer (pH 5.5) to give a homogenous suspension with a final DNA concentration of 2 mg/ml for intranasal administration to rabbits.

Male New Zealand white rabbits with an average weight of 2 kg, fed a regular diet, were randomly divided into four groups ($n = 8$ per group). One of the groups did not receive any treatment (normal group). The other three groups received intranasal administration of 5 kDa chitosan-based polyplexes (LMWC/DNA group), 173 kDa chitosan-based polyplexes (HMWC/DNA group), and saline (saline control group), respectively. Rabbits in LMWC/DNA and HMWC/DNA groups received DNA dose of 400 μg in 200 μl (100 μl each nostril). The rabbits were immunized at weeks 1, 4, 8, 12, 16 and 21. From week 15, all rabbits except those in the normal group were fed a high-fat/cholesterol diet consisting of 0.4 g cholesterol and 4 g saturated fatty acid per day for 13 weeks. Blood samples were collected during weeks 3, 7, 11, 15, 19, 24 and 28 for analyses of anti-CETP IgG as well as lipids and lipoproteins. After rabbits were killed at week 28, aortas were harvested for observation of atherosclerotic lesion.

2.9. ELISA assay of serum anti-CETP antibodies

The anti-CETP antibodies in serum were determined using recombinant human vascular endothelial growth factor-CETPC (rhVEGF-CETPC) by ELISA. Purified rhVEGF-CETPC was diluted in 0.05 mM carbonate–bicarbonate buffer (pH 9.6), then added to ELISA plates (Costar, USA) at 100 μl per well and incubated overnight at 4 °C. The plates were blocked with PBS containing 5% bovine serum albumin (BSA, Sigma, USA) for 2 h at 37 °C after discarding the coating solution, and then incubated with 100 μl of the serum samples (diluted to 1:100 with PBS containing 2% BSA) from the immunized animals. After incubating for 1 h at 37 °C, the wells were washed with PBS containing 0.1% Tween-20, then incubated with 100 μl goat anti-rabbit IgG horseradish peroxidase (HRP) (diluted to 1:20,000 with PBS containing 2% BSA) for 1 h at 37 °C. The wells were intensively washed with PBS containing 0.1% Tween-20, then incubated for 15 min with 50 μl of 0.01% 3,3′,5,5′-tetramethylbenzidine solution and 50 μl of 0.24% H_2O_2-urea solubilized in 0.2 M Na_2HPO_4–0.1 M citrate buffer (pH 5.5) at 37 °C. The reaction was stopped by addition of 50 μl 2 M H_2SO_4, and the $OD_{450\,nm}$ value was measured.

2.10. Western blot analysis of anti-CETP antibodies

The specific IgG antibodies against CETP were further investigated using Western blot analysis. Purified rhVEGF-CETPC in the presence and absence of DL-dithiothreitol (DTT) and rhVEGF reduced with DTT were run in a 15% SDS-PAGE gel under denaturing conditions and transferred to nitrocellulose membrane (Millipore Corp, USA). The membrane was blocked with 5% BSA in Tris-buffered saline (TBS, pH 7.5; 100 mM Tris–HCl, 0.9% NaCl) for 2 h at room temperature. Serum samples from immunized rabbits in LMWC/DNA group were diluted to 1:20 with TBS containing 5% BSA and then hybridized with proteins on the membrane for 1 h at 37 °C. The membrane was washed four times in TTBS (TBS with 0.1% Tween-20) and developed with HRP-conjugated goat anti-rabbit IgG (diluted to 1:200 with TBS containing 5% BSA). After washing four times with TTBS, the reaction was developed using 0.05% 3,3′-diaminobenzidine and 0.012% H_2O_2 in 10 mM Tris–HCl buffer (pH 7.5) at 37 °C for 15 min.

2.11. Analysis of plasma lipids and lipoproteins

The concentrations of TC, HDL-C and LDL-C of each rabbit were determined at week 28 by commercial kits (Wako, Japan) as instructed by the manufacturer to analyze the effects of anti-CETP antibodies on the plasma lipids concentration and lipoproteins distribution.

2.12. Observation of aortic atherosclerotic lesions

Contrary to the normal aorta, cholesterol-rich aorta could be easily stained by Sudan III. The aortas, from the aortic valve to the iliac bifurcation, were collected and stained with 0.2% (w/v) Sudan III in 75% ethanol to visualize the areas of lipid deposition. After washing with 70% ethanol (v/v), the opened aortas were immobilized by adhesive tapes and then the lumens were scanned into TIFF figures by a scanner. The magnitude of Sudan III-staining area in the entire aortic area was calculated by Mapinfo Professional 7.0 (Mapinfo Corporation, USA).

2.13. Interaction of chitosan/DNA polyplexes with nasal mucosa

The chitosan and DNA were labeled with RBITC and FITC, respectively. The transport of double-labeled chitosan/DNA polyplexes across nasal epithelium was investigated by CLSM.

2.13.1. Preparation of FITC-DNA

FITC-DNA was synthesized according to the diazonium-reaction as previously described (Ishii et al., 2000). Briefly, fluorescein isothiocyanate was reacted with equal mole of 2-(4-aminophenyl)-ethylamine in dimethyl-formamide overnight under stirring at 25 °C. The formation of FITC-aniline was monitored by thin layer chromatography with an eluent consisting of hexane/ethyl acetate (2:8, v/v) until the detection of single mark at $R_f = 0.26$. Subsequently, the FITC-aniline was reacted with sodium nitrite in HCl (0.5 M) at 0 °C under stirring for 5 min. The reaction was stopped by the addition of 1 M NaOH, and the solution obtained was mixed with DNA in 0.1 M borate buffer (pH 9.0) at 25 °C under stirring for

Table 1
Characterization of chitosan/DNA polyplexes prepared with chitosans of different MW (mean ± S.D., $n = 3$).

Chitosan MW (kDa)	Particle size (nm)	Zeta potential (mV)	Association efficiency (%)
5	800 ± 200	18.0 ± 1.1	87.9 ± 1.6
8	740 ± 100	17.8 ± 0.9	90.4 ± 2.5
32	220 ± 30	18.7 ± 2.3	95.0 ± 2.8
173	240 ± 20	20.4 ± 0.8	95.8 ± 1.8
425	250 ± 10	20.1 ± 1.2	96.7 ± 2.4

30 min. FITC-DNA was isolated by ethanol precipitation. The precipitate was washed extensively with ethanol until there was no free FITC fluorescence signal in ethanol.

2.13.2. Preparation of RBITC-chitosan

Chitosan was labeled with RBITC by the reaction between the isothiocyanate group of RBITC and the primary amine group of the chitosan (Wang et al., 2006). Firstly, the chitosan was dissolved in acetate buffer (pH 5.5) to 10 mg/ml, and the RBITC, dissolved in methanol at 2 mg/ml concentration, was added to the chitosan solution. The reaction mixture was stirred for 24 h in the dark at room temperature and then dialyzed with 0.1% acetic acid. Finally, the RBITC-labeled chitosan was obtained by freeze-drying.

2.13.3. Transport of chitosan/DNA polyplexes across the nasal epithelium

The double-labeled polyplexes were prepared with RBITC-chitosan and FITC-DNA as described above. Male Sprague–Dawley rats (250–300 g) were surgically treated according to the method of Hirai et al. (1981). Briefly, rats were anesthetized using urethane and placed in a supine position on a heated working surface. A cannula was then inserted into the trachea to maintain respiration. Another tube used to perfuse solution into the nasal cavity was inserted through the esophagus to the posterior part of the nasal cavity. The nasopalatine duct was sealed with medical glue to prevent drainage of the test solution from the nasal cavity into the mouth. Then, double-labeled polyplexes suspension or FITC-DNA in PBS was placed in a beaker and circulated through the nasal cavity at 37 °C for 1 or 2 h. Finally, the animals were sacrificed and their nasal mucosa was carefully excised. The nasal mucosa was observed by CLSM (LSM510, Carl Zeiss, Germany).

2.14. Statistical analysis

Data obtained were expressed as mean ± standard deviation (S.D.) and analyzed by Student's *t*-test. A difference between mean values was considered to be significant if $p < 0.05$.

3. Results

3.1. Characterization of chitosan/DNA polyplexes

The particle size, zeta potential and association efficiency of the polyplexes were shown in Table 1. In the polyplexes prepared with HMWCs (32, 173, and 425 kDa), a narrow particle size ranging from 220 to 250 nm was detected. However, the polyplexes prepared with LMWCs (5 and 8 kDa) had a larger particle size of above 740 nm in average. The five polyplexes exhibited similar zeta potentials ranging from 17.8 to 20.4 mV, suggesting that the polyplexes were positively charged. The association efficiencies of approximately 100% were obtained with the HMWCs-based polyplexes, while lower association efficiencies of about 90% were found in the LMWCs-based polyplexes.

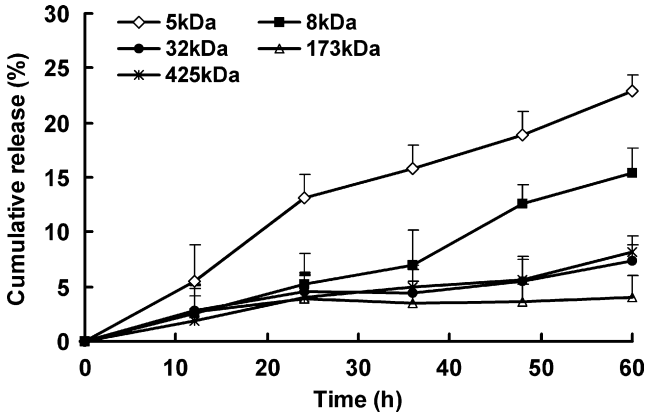

Fig. 1. DNA release curves of the polyplexes prepared with chitosans of various MW in PBS (mean ± S.D., $n = 4$).

3.2. In vitro release of DNA

The *in vitro* DNA release profile from the polyplexes was shown in Fig. 1. There existed a slow release of DNA in a 60 h period in all the polyplexes. The cumulative release of polyplexes prepared with HMWCs (32, 173, and 425 kDa) was less than 9% at 60 h, and there was no significant difference among the three HMWC-based polyplexes. However, there was a relatively rapid release of DNA from the polyplexes prepared with LMWCs, with the cumulative releases of 15% and 23% by 8 and 5 kDa chitosan-based polyplexes at 60 h, respectively.

3.3. Gel retardation assay

Chitosan could condense DNA to form polyplexes by neutralizing the negative charges on the phosphate backbone of DNA, thus retarding DNA mobility on the gel. As shown in Fig. 2, the migration of naked DNA toward the anode was observed in lane 1. The HMWC-based polyplexes (32, 173, and 425 kDa) effectively retarded DNA in the loading wells (Fig. 2, lanes 3–5). However, only slight retardation of DNA from migration was observed for 5 kDa chitosan-based polyplexes (Fig. 2, lane 2). It is thought that the weaker binding affinity of 5 kDa chitosan with DNA was responsible for the major dissociation of the polyplexes and mobility of DNA under applied electric field.

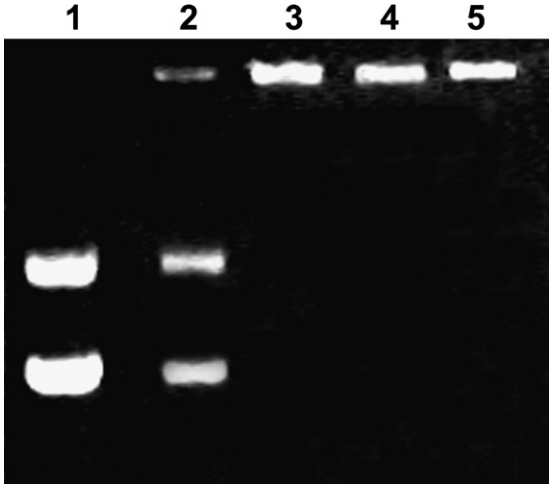

Fig. 2. Gel retarding analysis of chitosan/DNA polyplexes. Lane 1: naked DNA; lanes 2–5: polyplexes prepared with chitosans of 5, 32, 173 and 425 kDa, respectively.

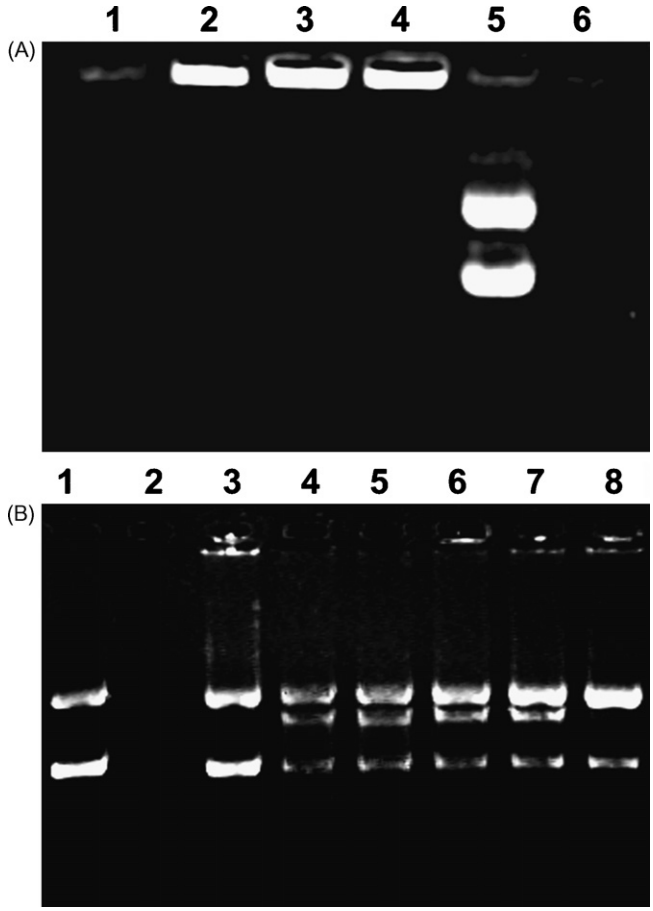

Fig. 3. Electrophoretic mobility analysis of chitosan/DNA polyplexes following DNase I digestion. (A) Naked DNA and polyplexes prepared with different MW chitosans were incubated with DNase I of 60 unit/ml. Lane 1: polyplexes (5 kDa) + DNase I; lane 2: polyplexes (32 kDa) + DNase I; lane 3: polyplexes (173 kDa) + DNase I; lane 4: polyplexes (425 kDa) + DNase I; lane 5: naked DNA; lane 6: naked DNA + DNase I. (B) Polyplexes prepared with 5 kDa chitosan were incubated with DNase I of different concentrations. Lane 1: naked DNA; lane 2: naked DNA + DNase I (5 unit/ml); lane 3: polyplexes; lane 4: polyplexes + DNase I (25 unit/ml); lane 5: polyplexes + DNase I (20 unit/ml); lane 6: polyplexes + DNase I (15 unit/ml); lane 7: polyplexes + DNase I (10 unit/ml); lane 8: polyplexes + DNase I (5 unit/ml).

3.4. DNase I protection assay

The effects of different MW chitosan on protection of DNA from enzymatic degradation were shown in Fig. 3A. When incubated with 60 unit/ml of DNase I at 37 °C for 30 min, the naked DNA was completely degraded leading to complete disappearance of fluorescent band of DNA (Fig. 3A, lane 6). At the same time, the polyplexes prepared with HMWCs (32, 173 or 425 kDa) were fully retained in the loading wells (Fig. 3A, lanes 2–4) and intense fluorescent bands occurred. It was evident that effective protection of DNA was imparted by these HMWCs. However, no fluorescent band was observed in the loading well (Fig. 3A, lane 1), which meant that 5 kDa chitosan failed to protect DNA from degradation when incubated with DNase I of 60 unit/ml.

A further experiment was carried out to evaluate the effect of 5 kDa chitosan on protection of DNA against DNase I degradation. The 5 kDa chitosan-based polyplexes were incubated with serial concentrations of DNase I at 37 °C for 30 min. As shown in Fig. 3B, naked DNA was completely degraded upon incubation with 5 unit/ml DNase I (Fig. 3B, lane 2). When the polyplexes treated with DNase I of 25, 20, 15, 10 and 5 unit/ml respectively, the fluorescent bands of migrated DNA were visualized in lanes 4–8 of the agarose gel, which was similar to the polyplexes untreated with DNase I (Fig. 3B, lane 3). Moreover, the fluorescence intensity attenuated with the increase of enzyme concentration, implicating partial degradation of the DNA. The result showed that the 5 kDa chitosan-based polyplexes could protect DNA from DNase I degradation in concentrations of 5–25 unit/ml. But incomplete protection of DNA against degradation took place when DNase I concentration was ≥10 unit/ml. In addition, the 5 kDa chitosan-based polyplexes dissociated and DNA migrated toward the anode under applied electric field, suggesting the weaker binding affinity of 5 kDa chitosan to DNA.

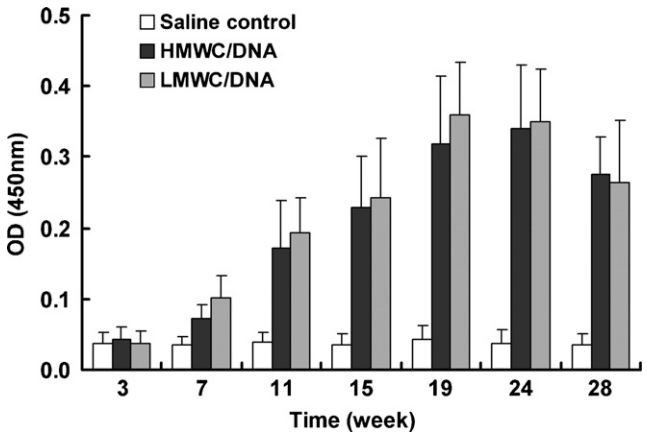

Fig. 4. The serum anti-CETP antibody levels of rabbits. Rabbits were intranasally immunized with HMWC/DNA polyplexes (173 kDa) or LMWC/DNA polyplexes (5 kDa) at weeks 1, 4, 8, 12, 16 and 21. Rabbits treated with saline were used as control. The serum samples were collected at weeks 3, 7, 11, 15, 19, 24, 28 and assayed by ELISA (mean ± S.D., $n = 8$).

3.5. In vitro transfection efficiency

The effect of chitosan on transfection efficiency was evaluated by varying MW of chitosan. The results showed that all chitosans mediated expression of green fluorescent protein in HEK293 cells. The transfection efficiencies for polyplexes prepared with chitosans of 32, 173, and 425 kDa were 17.1 ± 3.1%, 15.6 ± 2.5%, and 16.3 ± 1.8%, respectively. On the other hand, a higher transfection efficiency of 29.3 ± 5.8% was obtained for polyplexes prepared with the 5 kDa chitosan, which was approximately twice as much as that observed in the high MW ones ($p < 0.05$). As expected, naked DNA resulted in no detectable expression of green fluorescent protein.

3.6. Serum anti-CETP antibodies in rabbits

The anti-CETP antibodies in serum detected by ELISA are shown in Fig. 4. As compared with the saline control group, higher levels of anti-CETP IgG were induced in LMWC/DNA and HMWC/DNA group after the second intranasal administration and lasted from weeks 7 to 28. The IgG titres increased gradually over time, and then slightly fell at week 28. Comparison of the two groups of rabbits immunized with different polyplexes indicated that the data of anti-CETP IgG in the LMWC/DNA group were slightly higher than those in the HMWC/DNA group at each interval from weeks 7 to 24. However, there was no statistically significant difference ($p > 0.05$).

3.7. Western blot analysis of specific antibodies against CETP

VEGF is a homodimeric protein with intermolecular disulfide bonds. When analyzed in SDS-PAGE, VEGF would show a single band in the presence of reducing agents, and two bands without reducing agents. In-frame fusion of CETPC to VEGF does not deter the ability of VEGF to form homodimeric fusion protein. The

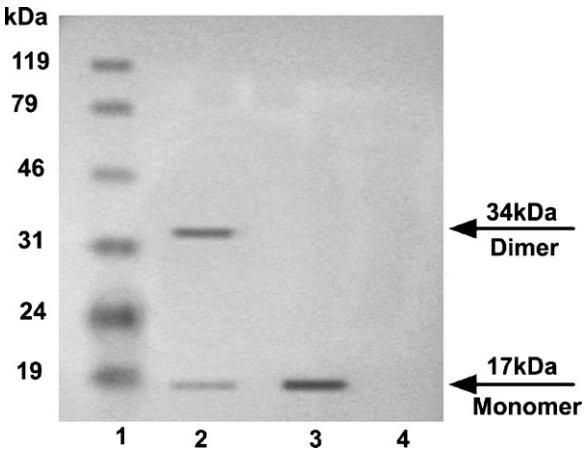

Fig. 5. Specificity of anti-CETP antibodies by Western blot analysis. To determine the specificity of anti-CETP antibodies produced in rabbits intranasally immunized with LMWC/DNA polyplexes (5 kDa), serum samples were tested by Western blot analysis using rhVEGF-CETPC fusion protein as antigen in the presence or absence of DTT. Lane 1: prestained protein molecular marker; lane 2: rhVEGF-CETPC reduced with DTT; lane 3: rhVEGF-CETPC without DTT; lane 4: rhVEGF without DTT.

protein band of the monomeric rhVEGF-CETPC "shifted" after partially folding into a homodimeric fusion protein under non-reducing conditions (Gaofu et al., 2005). This characteristic of rhVEGF-CETPC was used to determine the specificity of anti-CETP antibodies produced in immunized animals. Fig. 5 shows that the sera from rabbits of the LMWC/DNA group bound the rhVEGF-CETPC monomer (17 kDa, Fig. 5, lanes 2 and 3) and dimer (34 kDa, Fig. 5, lane 3), but not rhVEGF alone (Fig. 5, lane 4). The results further verified that the intranasal immunization of LMWC/DNA polyplexes could elicit specific antibodies against CETP and the antigenicity of the CETP vaccine was not altered following its complexation with LMWC.

3.8. Analysis of plasma lipids and lipoproteins

The levels of TC, HDL-C and LDL-C in plasma were determined by the commercial kits. The results were shown in Table 2. The levels of TC, HDL-C and LDL-C in the saline group fed with a high-cholesterol diet for 13 weeks were significantly higher than the normal group fed with a regular diet ($p < 0.01$), indicating the establishment of a high-cholesterol rabbit model. There existed significant decreases in plasma TC and LDL-C in the LMWC/DNA group compared with the saline group ($p < 0.01$), and the plasma HDL-C in the LMWC/DNA group was similar to those in the saline group ($p > 0.05$). There were no significant differences between the LMWC/DNA group and the HMWC/DNA group regarding to the levels of plasma TC, HDL-C and LDL-C ($p > 0.05$).

The ratio of HDL-C to TC (HDL-C/TC) and LDL-C to TC (LDL-C/TC) were used to describe the trend of plasma cholesterol in rabbits. The results indicated that the antiatherogenic HDL-C/TC was 100% higher in the LMWC/DNA group than in the saline control group ($34 \pm 6\%$ versus $17 \pm 6\%$, $p < 0.01$) and 76% higher in the HMWC/DNA group than in the saline control group ($30 \pm 10\%$ versus $17 \pm 6\%$, $p < 0.01$). The proatherogenic LDL-C/TC was 19% lower in the LMWC/DNA group than in the saline control group ($57 \pm 7\%$ versus $70 \pm 8\%$, $p < 0.05$) and 14% lower in the HMWC/DNA group than in the saline control group ($60 \pm 10\%$ versus $70 \pm 8\%$, $p > 0.05$). However, there were no significant differences between the LMWC/DNA group and the HMWC/DNA group regarding to the HDL-C/TC and LDL-C/TC ($p > 0.05$). In addition, the atherogenic index (ratio of non-HDL-C to HDL-C) was used to predict the development of atherosclerosis (Kwon et al., 2003). In this study, this index was adopted to assess the effectiveness in immunization. It was shown that the atherogenic index in the LMWC/DNA group was significantly lower than that in the saline controls (2.0 ± 0.5 versus 6 ± 3, $p < 0.01$). There was no significant difference between the groups of the LMWC/DNA and the HMWC/DNA (2.0 ± 0.5 versus 2 ± 1, $p > 0.05$).

3.9. Observation of aortic atherosclerotic lesions

Typical images of the aorta of rabbits stained with Sudan III were shown in Fig. 6. A marked lipid deposition accompanied by continuous plaque formation was observed in the aortas from the saline control group, and the average percentage of aortic area covered by atherosclerotic lesion in the entire aorta area was as high as $71 \pm 14\%$ (Fig. 6A). However, the area of aortic lesions and intimal thickening were greatly reduced in the LMWC/DNA compared with those in the aortas from the rabbits treated with saline. It was observed that the percentage of aortic lesions area in the LMWC/DNA group decreased by 51% than saline controls ($35 \pm 18\%$ versus $71 \pm 14\%$, $p < 0.01$), and it was similar to that of the HMWC/DNA group ($35 \pm 18\%$ versus $29 \pm 11.0\%$, $p > 0.05$). The imaging analysis of aortic area suggested that intranasal immunization with chitosan/DNA polyplexes could significantly inhibit the progression of atherosclerosis (mean ± S.D., $n = 8$).

3.10. Interaction of chitosan/DNA polyplexes with the nasal mucosa

With the purpose of investigating the interaction of chitosan/DNA polyplexes with the nasal mucosa, the double-labeled RBITC-chitosan/FITC-DNA polyplexes and FITC-DNA solution were administered intranasally to rats respectively, and the transport of polyplexes and DNA across the nasal mucosa was monitored by CLSM. The x, z and y, z sections taken 15 μm underneath the mucosal surface were selected for analysis at 2 h after nasal administration (Fig. 7). As indicated by the orange fluorescence in the nasal

Table 2
Effects of intranasal immunization with chitosan/DNA polyplexes prepared with LMWC or HMWC on plasma lipids in cholesterol-fed rabbits (mean ± S.D., $n = 8$).

Group	TC (mM)	HDL-C (mM)	LDL-C (mM)	HDL-C/TC (%)	LDL-C/TC (%)	Atherogenic index
Normal	1.0 ± 0.3	0.5 ± 0.1	0.3 ± 0.1	60 ± 20	27 ± 6	0.9 ± 0.4
Saline control	48 ± 7[a]	8 ± 3[a]	33 ± 6[a]	17 ± 6[a]	70 ± 8[a]	6 ± 3[a]
LMWC/DNA	23 ± 6[b,c]	8 ± 1[d,c]	13 ± 4[b,c]	34 ± 6[b,c]	57 ± 7[e,c]	2.0 ± 0.5[b,c]
HMWC/DNA	30 ± 10[b]	8 ± 2[d]	16 ± 8[b]	30 ± 10[b]	60 ± 10[d]	2 ± 1[e]

The blood samples from each group were collected at week 28, and the levels of TC, HDL-C and LDL-C in plasma were determined by commercial kits. Values are mean ± S.D. TC, total cholesterol; HDL-C, high density lipoprotein cholesterol; LDL-C, low density lipoprotein cholesterol; Atherogenic index, ratio of non-HDL-C to HDL-C.

[a] Differences (t-test) are $p < 0.01$ *vs.* normal group.
[b] Differences (t-test) are $p < 0.01$ *vs.* saline control group.
[c] Differences (t-test) are $p > 0.05$ *vs.* HMWC/DNA group.
[d] Differences (t-test) are $p > 0.05$ *vs.* saline control group.
[e] Differences (t-test) are $p < 0.05$ *vs.* saline control group.

Fig. 6. Typical photographs of lesions in aortas from cholesterol-fed rabbits intranasally administered with saline (A), HMWC/DNA polyplexes (173 kDa) (B), and LMWC/DNA polyplexes (5 kDa) (C).

mucosa treated with double-labeled polyplexes prepared with either 5 or 173 kDa chitosan (Fig. 7B and C), the polyplexes were internalized into the mucosal epithelia and, further transported into deeper regions of the subepithelial area. On the contrary, no green fluorescence was observed in the rat nasal mucosa treated with FITC-DNA solution (Fig. 7A), which provides evidence that the uptake of naked DNA in the nasal mucosa was negligible.

Fig. 8 was the Z-scan fluorescence images (20 images), in successive steps (1.5 μm distance between steps), of the nasal mucosa from the apical side to the depth of 30 μm beneath the mucosal epithelia treated with double-labeled 5 kDa-based polyplexes. The images showed that both the depth of penetration and the amount of the polyplexes increased over time. The polyplexes were gradually transported into all depths of the mucosa (up to 30 μm) at

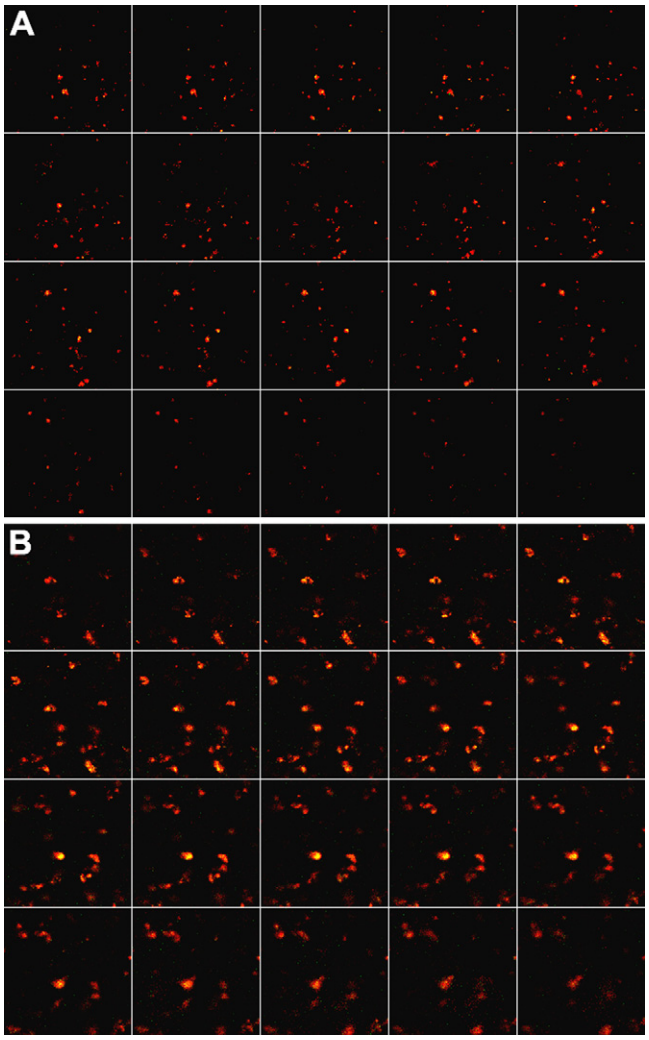

Fig. 8. Z-scan images of the rat nasal mucosa from the apical side to depth of 30 μm beneath mucosa. The rat nasal mucosa was treated with RBITC-chitosan/FITC-DNA polyplexes prepared with 5 kDa chitosan for 1 h (A) and 2 h (B). The 20 images were in successive steps with 1.5 μm apart.

2 h after administration. The images all showed that DNA in a complex form associated with 5 kDa chitosan was transported across mucosa.

To better understand the effect of chitosan MW on the transport of chitosan/DNA polyplexes across nasal epithelium, the rat nasal

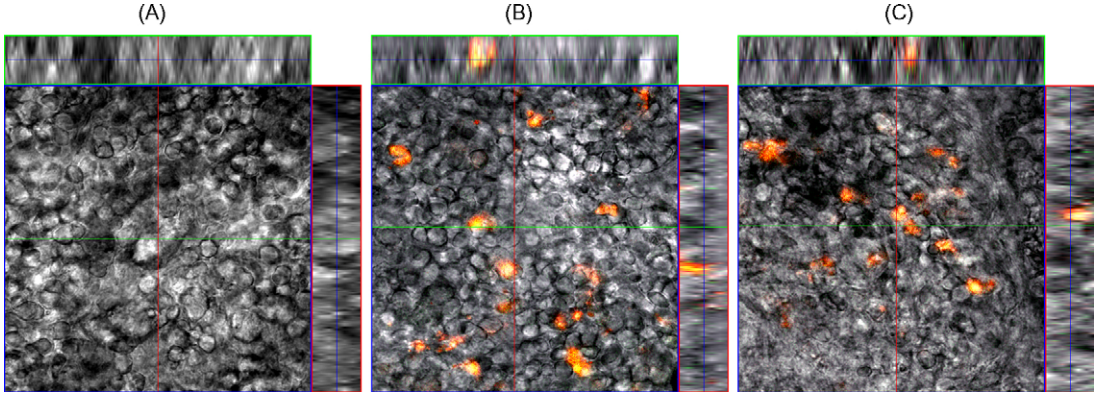

Fig. 7. CLSM images of the x, z and y, z sections taken 15 μm inside the mucosa from the apical side. The rat nasal mucosa was treated for 2 h with FITC-DNA solution (A), RBITC-chitosan/FITC-DNA polyplexes based on 5 kDa chitosan (B), and RBITC-chitosan/FITC-DNA polyplexes based on 173 kDa chitosan (C). The sections were taken 15 μm underneath the mucosa surface.

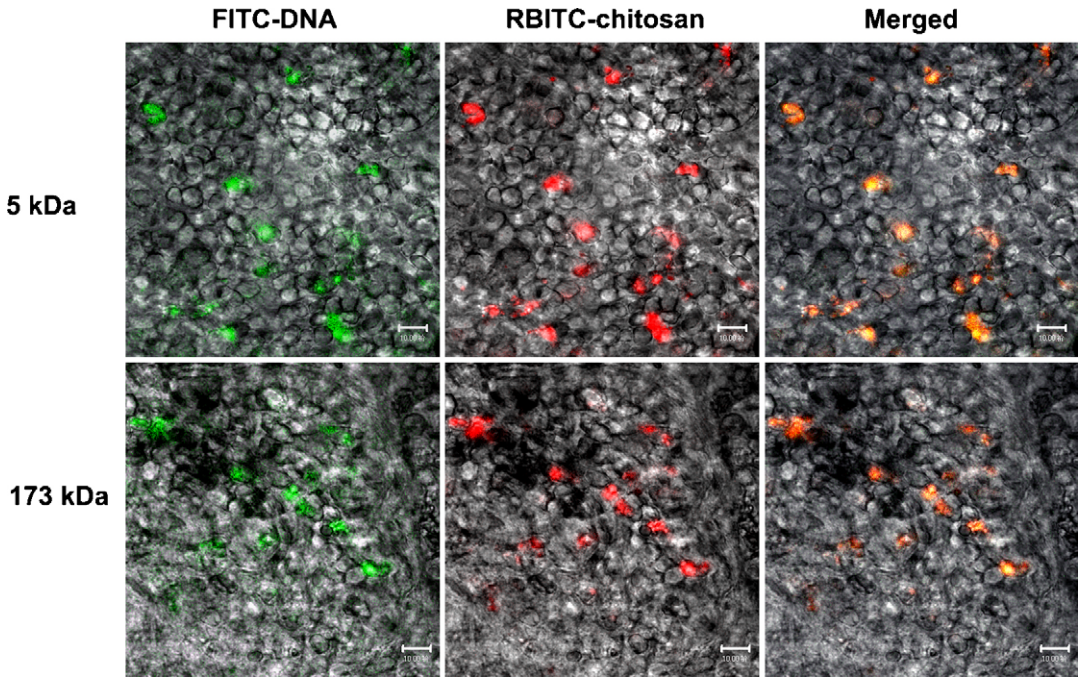

Fig. 9. CLSM images of cross-section taken 15 μm inside the mucosa from the apical side. The rat nasal mucosa was treated with FITC-DNA, RBITC-chitosan and RBITC-chitosan/FITC-DNA polyplexes (merged) for 2 h, respectively. The polyplexes were prepared with 5 or 173 kDa chitosan. Scale bar is 10 μm.

mucosa was treated for 2 h with double-labeled polyplexes prepared with either 5 or 173 kDa chitosan, and the CLSM images of cross-sections taken at the depth of 15 μm underneath the mucosa surface were showed in Fig. 9. It was clear that the green fluorescence corresponding to FITC-DNA were strictly co-localized with the red fluorescence corresponding to RBTIC-chitosan and the merged image exhibited orange fluorescence, indicating that DNA remained complexed with chitosan inside the nasal mucosa. The results showed that regardless of the MW of chitosan, the polyplexes did not dissociate upon contact with the nasal mucosa and the LMWC-based polyplexes were stable during the process of transepithelial transport.

4. Discussion

LMWCs are more advantageous in gene delivery than HMWCs because of their better biodegradability and lower cytotoxicity. However, until now, little has been done on *in vivo* efficacy of LMWCs-based DNA delivery. In the present study, we examined *in vitro* properties and *in vivo* efficiency of LMWCs as gene carriers.

It is necessary to understand how chitosan MW affects the physicochemical properties of chitosan/DNA polyplexes. It is known that aqueous solubility of chitosan is related to MW. LMWCs (5 and 8 kDa) are aqueous soluble, while HMWCs (32, 173, and 425 kDa), due to their high degree of polymerization, are insoluble at neutral pH but soluble at acidic pH. In the present study, the polyplexes prepared with 32, 173, and 425 kDa chitosans were characterized with smaller particle size and nearly 100% association efficiency, while the polyplexes prepared with LMWCs (5 and 8 kDa) had a larger particle size with a lower association efficiency. The *in vitro* release showed that the LMWCs-based polyplexes tended to dissociate and release DNA. The influence of chitosan MW on formation of the polyplexes could be explained by the chain entanglement effect (Kiang et al., 2004). Compared with HMWCs, LMWCs condensed DNA less efficiently at the same N/P ratio as a result of their shorter polymer chain and lower entanglement capability. Consequently, the LMWCs-based polyplexes with a larger size and lower association efficiency were formed. The relationship between chitosan MW and the binding ability of chitosan to DNA was further confirmed by the gel retardation assay. It was shown that the polyplexes prepared with LMWCs were dissociated and the DNA migrated out of the loading well under applied external force, while there was no dissociation for the polyplexes prepared with HMWCs under the force. As a result, we believed that the reduction in the degree of polymerization resulted in reduced physical stability of LMWC polyplexes. Our findings concerning the effect of chitoan MW on the binding capacity of chitosan for DNA and the properties of polyplexes were also consistent with the results obtained by Huang et al. (2005) and Lavertu et al. (2006).

The present results indicated that the capacity of chitosan to protect the DNA from degradation is also related to the MW. The weaker binding affinity of LMWC to DNA resulted in the reduced protection of DNA. Moreover, it was found that DNA was undigested when the 5 kDa chitosan-based polyplexes were incubated with DNase I of 5 unit/ml, indicating that it could effectively protect DNA from DNase degradation at low concentrations. Although it is necessary for an effective gene delivery system to be stable to ensure the protection of DNA from extracellular nuclease, followed by endosomal–lysosomal escape (Borchard, 2001), the nuclear translocation and gene expression are not achieved unless DNA is released from the polyplexes once inside the cells (Schaffer et al., 2000). Thus, an appropriate balance between the stability of polyplexes and the intracellular release of DNA from these polyplexes has to be maintained to reach high-level gene expression. In view of the present transfection experiment, it was found that 5 kDa chitosan-based polyplexes achieved higher transfection efficiency, about twice than those observed with HMWCs. And it appeared that the HMWC-based polyplexes were more stable than the ones based on LMWC. We speculated that the strong affinity of HMWCs to DNA hindered DNA release from its carrier, which was regarded as a rate-limiting step for the intracellular release and nuclear entry of DNA, resulting in low transfection efficiency.

Recently, increasing attention has been directed toward the chemically modified low molecular weight chitosan. Hydrophobically modified chitosans, for example, low MW chitosan grafted with N-/2(3)-(dodec-2-enyl) succinoyl groups (Zhang et al., 2008)

and deoxycholic acid-conjugated chitosan oligosaccharide (Chae et al., 2005b), facilitate bilayer permeabilization, leading to the enhanced uptake by the target cells. Chitosan oligomer was modified with urocanic acid bearing imidazole ring which could play the role in the osmotic rupture of endosome, which promoted the cytosolic release of polyplexes (Wang et al., 2008). Chitosan oligomers coupled with ligand were able to bind to receptors on specific cell lines, offering the potential to target specific cells (Kim et al., 2004, 2006). Chemical modified LMWCs-based polyplexes with better performances could overcome specific gene delivery barriers, thereby enhancing gene transfection efficiency.

To investigate the effect of chitosan MW on *in vivo* gene delivery efficiency, a 28-week immunotherapy in rabbits intranasally immunized with LMWC- and HMWC-based polyplexes was initiated. The results indicated that nasal vaccination of LMWC/DNA polyplexes elicited specific anti-CETP IgG antibodies whose presence lasted for more than 21 weeks. In addition, the analysis of plasma lipids and lipoproteins showed that the antiatherogenic HDL-C/TC was increased and proatherogenic LDL-C/TC was decreased in the LMWC/DNA group when compared to those of the saline group. The observation from the aortas revealed that the areas of atherosclerotic plaques were remarkably reduced in the LMWC/DNA group if compared with those in the aortas from the rabbits treated with saline. The present results showed that LMWC appears as an efficient carrier for DNA delivery via mucosa. Furthermore, *in vivo* studies showed that there were no significant differences between the HMWC/DNA group and LMWC/DNA group with regard to the level of anti-CETP antibodies, the plasma lipoprotein profile and the area of atherosclerotic plaques. However, this is not in agreement with the observation of *in vitro* transfection efficiency produced by the HMWC/DNA group. Regarding the discrepancy, we suppose that it could be attributed to the cumulative effect of the sustained-release of DNA from the HMWC/DNA polyplexes in the period of 6-month immunization, thereby resulting in the attentuated effect of chitosan MW on *in vivo* gene expression. The reasons behind the observation perhaps need further exploration.

Following intranasal administration, the initiation of immune response depends on the ability of vaccine to cross the mucosal epithelial barrier and to be presented by the antigen presenting cells. Van der Lubben et al. performed a preliminary study on *in vivo* uptake of chitosan microparticles via oral vaccination in mice, which proved that chitosan microparticles were taken up by M-cells of Peyer's patches (van der Lubben et al., 2001). It was also found that the specialized epithelial cells, which are morphologically similar to the intestinal M-cells, exist in the nasal epithelium (Gebert, 1995) and are capable of internalizing particles (Fujimura et al., 2006). The CLSM images of the nasal mucosa treated with polyplexes exhibited that the penetration of DNA across the nasal epithelia was enhanced by its complexation with chitosan. Although the present results showed that LMWC/DNA polyplexes released DNA more easily than did HMWC/DNA polyplexes, they were sufficiently stable during the process of the submucosal penetration. Irrespective of the MW of chitosan (5 kDa or 173 kDa), the polyplexes could be internalized by the nasal epithelial cells and transported to the cell layers underneath. The observation showed that chitosan MW had no influence on the transport behavior of polyplexes, which was consistent with the enhanced system immune responses induced by the LMWC/DNA or HMWC/DNA polyplexes. However, more in-depth studies should be done to unveil the intramucosal transport mechanism of DNA mediated by chitosan as well as the influence of chitosan MW on the process of transport.

In view of the above results, it is concluded that LMWC is capable of shuttling DNA vaccines across the nasal mucosa and that the LMWC-based polyplexes could elicit an enhanced systemic immune response against the encoded protein. Although differences in their *in vitro* properties were observed, LMWC and HMWC-based polyplexes showed similar effectiveness *in vivo*. The LMWCs have the potential as carriers for the mucosal delivery of DNA vaccine.

Acknowledgements

This work was supported by China National Natural Science Fund Committee (Grants 30371698, 30500458 and 30572272).

References

Barter, P.J., Kastelein, J.J., 2006. Targeting cholesteryl ester transfer protein for the prevention and management of cardiovascular disease. J. Am. Coll. Cardiol. 47, 492–499.
Bivas-Benita, M., van Meijgaarden, K.E., Franken, K.L., Junginger, H.E., Borchard, G., Ottenhoff, T.H., Geluk, A., 2004. Pulmonary delivery of chitosan-DNA nanoparticles enhances the immunogenicity of a DNA vaccine encoding HLA-A*0201-restricted T-cell epitopes of *Mycobacterium tuberculosis*. Vaccine 22, 1609–1615.
Borchard, G., 2001. Chitosans for gene delivery. Adv. Drug Deliv. Rev. 52, 145–150.
Carreño-Gómez, B., Duncan, R., 1997. Evaluation of the biological properties of soluble chitosan and chitosan microspheres. Int. J. Pharm. 148, 231–240.
Chae, S.Y., Jang, M.K., Nah, J.W., 2005a. Influence of molecular weight on oral absorption of water soluble chitosans. J. Control. Release 102, 383–394.
Chae, S.Y., Son, S., Lee, M., Jang, M.K., Nah, J.W., 2005b. Deoxycholic acid-conjugated chitosan oligosaccharide nanoparticles for efficient gene carrier. J. Control. Release 109, 330–344.
Fujimura, Y., Akisada, T., Harada, T., Haruma, K., 2006. Uptake of microparticles into the epithelium of human nasopharyngeal lymphoid tissue. Med. Mol. Morph. 39, 181–186.
Gaofu, Q., Jie, L., Rongyue, C., Xin, Y., Dan, M., Jie, W., Shen, X., Xu, Q., Rousel, S.Q., Zhao, X., Liu, J., 2005. Asparaginase display of polypeptides in the periplasm of *Escherichia coli*: potential rapid pepscan technique for antigen epitope mapping. J. Immunol. Methods 299, 9–19.
Gebert, A., 1995. Identification of M-cells in the rabbit tonsil by vimentin immunohistochemistry and *in vivo* protein transport. Histochem. Cell Biol. 104, 211–220.
Guliyeva, Ü., Öner, F., Özsoy, Ş., Haziroğlu, R., 2006. Chitosan microparticles containing plasmid DNA as potential oral gene delivery system. Eur. J. Pharm. Biopharm. 62, 17–25.
Hirai, S., Yashiki, T., Matsuzawa, T., Mima, H., 1981. Absorption of drugs from the nasal mucosa of rat. Int. J. Pharm. 7, 317–325.
Huang, M., Fong, C.W., Khor, E., Lim, L.Y., 2005. Transfection efficiency of chitosan vectors: effect of polymer molecular weight and degree of deacetylation. J. Control. Release 106, 391–406.
Ishii, T., Okahata, Y., Sato, T., Facile, 2000. Preparation of a fluorescence-labeled plasmid. Chem. Lett. 29, 386–387.
Khatri, K., Goyal, A.K., Gupta, P.N., Mishra, N., Vyas, S.P., 2008. Plasmid DNA loaded chitosan nanoparticles for nasal mucosal immunization against hepatitis B. Int. J. Pharm. 354, 235–241.
Kiang, T., Wen, J., Lim, H.W., Leong, K.W., 2004. The effect of the degree of chitosan deacetylation on the efficiency of gene transfection. Biomaterials 25, 5293–5301.
Kim, T.H., Park, I.K., Nah, J.W., Choi, Y.J., Cho, C.S., 2004. Galactosylated chitosan/DNA nanoparticles prepared using water-soluble chitosan as a gene carrier. Biomaterials 25, 3783–3792.
Kim, T.H., Jin, H., Kim, H.W., Cho, M.H., Cho, C.S., 2006. Mannosylated chitosan nanoparticle-based cytokine gene therapy suppressed cancer growth in BALB/c mice bearing CT-26 carcinoma cells. Mol. Cancer Ther. 5, 1723–1732.
Köping-Höggård, M., Mel'nikova, Y.S., Vårum, K.M., Lindman, B., Artursson, P., 2003. Relationship between the physical shape and the efficiency of oligomeric chitosan as a gene delivery system *in vitro* and *in vivo*. J. Gene Med. 5, 130–141.
Köping-Höggård, M., Vårum, K.M., Issa, M., Danielsen, S., Christensen, B.E., Stokke, B.T., 2004. Improved chitosan-mediated gene delivery based on easily dissociated chitosan polyplexes of highly defined chitosan oligomers. Gene Ther. 11, 1441–1452.
Kwon, M.J., Song, Y.S., Choi, M.S., Song, Y.O., 2003. Red pepper attenuates cholesteryl ester transfer protein activity and atherosclerosis in cholesterol-fed rabbits. Clin. Chim. Acta 332, 37–44.
Lavertu, M., Méthot, S., Tran-Khanh, N., Buschmann, M.D., 2006. High efficiency gene transfer using chitosan/DNA nanoparticles with specific combinations of molecular weight and degree of deacetylation. Biomaterials 27, 4815–4824.
Lee, M., Nah, J.W., Kwon, Y., Koh, J.J., Ko, K.S., Kim, S.W., 2001. Water-soluble and low molecular weight chitosan-based plasmid DNA delivery. Pharm. Res. 18, 427–431.
MacLaughlin, F.C., Mumper, R.J., Wang, J., Tagliaferri, J.M., Gill, I., Hinchcliffe, M., Alain, P.R., 1998. Chitosan and depolymerized chitosan oligomers as condensing carriers for *in vivo* plasmid delivery. J. Control. Release 56, 259–272.
Mansouri, S., Cuie, Y., Winnik, F., Shi, Q., Lavigne, P., Benderdour, M., Eric, B., Julio, C.F., 2006. Characterization of folate-chitosan-DNA nanoparticles for gene therapy. Biomaterials 27, 2060–2065.
Mao, D., Kai, G., Gaofu, Q., Zheng, Z., Li, Z., Jie, W., Jingjing, L., Rongyue, C., 2006. Intramuscular immunization with a DNA vaccine encoding a 26-amino acid CETP

epitope displayed by HBc protein and containing CpG DNA inhibits atherosclerosis in a rabbit model of atherosclerosis. Vaccine 24, 4942–4950.
Nakamura, F., Onishi, H., Machida, Y., Nagai, T., 1992. Lysozyme-catalyzed degradation properties of the conjugates between chitosans having some deacetylation degrees and methotrexate. Yakuzaigaku 52, 59–67.
Nilsson, J., Hansson, G.K., Shah, P.K., 2005. Immunomodulation of atherosclerosis: implications for vaccine development. Arterioscler. Thromb. Vasc. Biol. 25, 18–28.
Özgel, G., Akbuğa, J., 2006. *In vitro* characterization and transfection of IL-2 gene complexes. Int. J. Pharm. 315, 44–51.
Richardson, S.C., Kolbe, H.V., Duncan, R., 1999. Potential of low molecular mass chitosan as a DNA delivery system: biocompatibility, body distribution and ability to complex and protect DNA. Int. J. Pharm. 178, 231–243.
Romøren, K., Pedersen, S., Smistad, G., Evensen, Ø., Thu, B.J., 2003. The influence of formulation variables on in vitro transfection efficiency and physicochemical properties of chitosan-based polyplexes. Int. J. Pharm. 261, 115–127.
Schaffer, D.V., Fidelman, N.A., Dan, N., Lauffenburger, D.A., 2000. Vector unpacking as a potential barrier for receptor-mediated polyplex gene delivery. Biotechnol. Bioeng. 67, 598–606.
van der Lubben, I.M., Verhoef, J.C., van Aelst, A.C., Borchard, G., Junginger, H.E., 2001. Chitosan microparticles for oral vaccination: preparation, characterization and preliminary *in vivo* uptake studies in murine Peyer's patches. Biomaterials 22, 687–694.
Wang, B., Chen, K., Jiang, S., Reincke, F., Tong, W., Wang, D., Gao, C., 2006. Chitosan-mediated synthesis of gold nanoparticles on patterned poly (dimethylsiloxane) surfaces. Biomacromolecules 7, 1203–1209.
Wang, W., Yao, J., Zhou, J.P., Lu, Y., Wang, Y., Tao, L., Li, Y.P., 2008. Urocanic acid-modified chitosan-mediated p53 gene delivery inducing apoptosis of human hepatocellular carcinoma cell line HepG2 is involved in its antitumor effect *in vitro* and *in vivo*. Biochem. Biophys. Res. Commun. 377, 567–572.
Yuan, X., Yang, X., Cai, D., Mao, D., Wu, J., Zong, L., Liu, J., 2008. Intranasal immunization with chitosan/pCETP nanoparticles inhibits atherosclerosis in a rabbit model of atherosclerosis. Vaccine 26, 3727–3734.
Zhang, H., Cheng, C., Zheng, M., Chen, J.L., Meng, M.J., Zhao, Z.Z., Chen, Q., Xie, Z., Li, J.L., Yang, Y., Shen, Y., Wang, H.N., Wang, Z.Z., Gao, R., 2007. Enhancement of immunity to an *Escherichia coli* vaccine in mice orally inoculated with a fusion gene encoding porcine interleukin 4 and 6. Vaccine 25, 7094–7101.
Zhang, X., Ercelen, S., Duportail, G., Schaub, E., Tikhonov, V., Slita, A., Zarubaev, V., Babak, V., Mély, Y., 2008. Hydrophobically modified low molecular weight chitosans as efficient and nontoxic gene delivery vectors. J. Gene Med. 10, 527–539.
Zhao, X., Yu, S.B., Wu, F.L., Mao, Z.B., Yu, C.L., 2006. Transfection of primary chondrocytes using chitosan-pEGFP nanoparticles. J. Control. Release 112, 223–228.